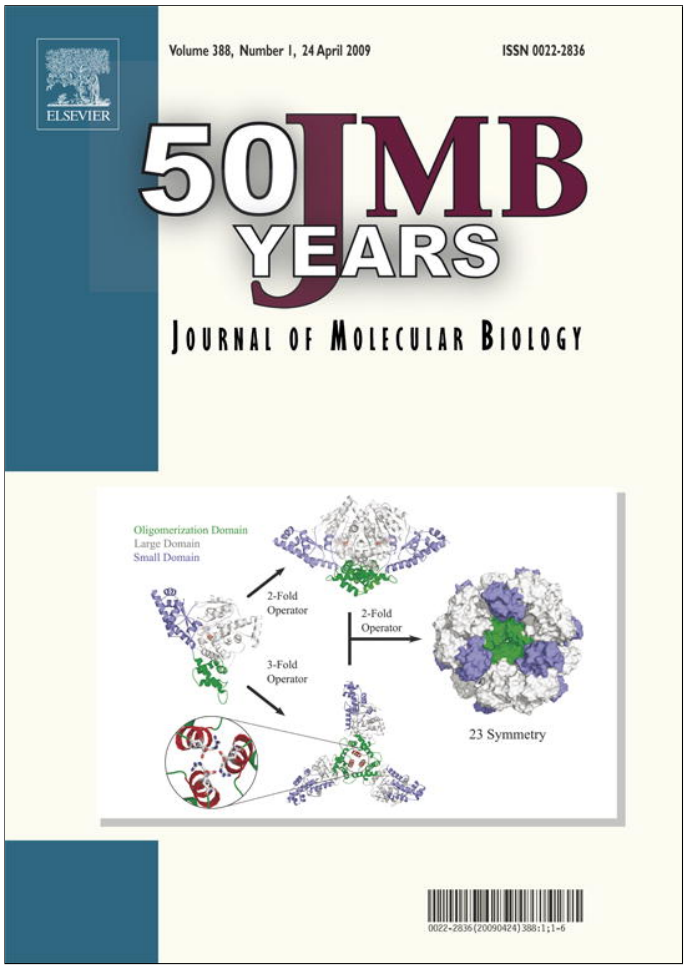

doi:10.1016/j.jmb.2009.03.005 J. Mol. Biol. (2009) 388, 133–143

JMB

Available online at www.sciencedirect.com

ScienceDirect

ELSEVIER

Desmin and Vimentin Intermediate Filament Networks: Their Viscoelastic Properties Investigated by Mechanical Rheometry

Michael Schopferer[1]†, Harald Bär[2,3]†, Bernhard Hochstein[1], Sarika Sharma[2,3], Norbert Mücke[4], Harald Herrmann[3] and Norbert Willenbacher[1]*

[1]*Institute of Mechanical Process Engineering and Mechanics, University of Karlsruhe, 76131 Karlsruhe, Germany*

[2]*Department of Cardiology, University of Heidelberg, 69120 Heidelberg, Germany*

[3]*Department of Molecular Genetics, German Cancer Research Center, 69120 Heidelberg, Germany*

[4]*Department of Biophysics of Macromolecules, German Cancer Research Center, 69120 Heidelberg, Germany*

Received 16 December 2008; received in revised form 2 March 2009; accepted 3 March 2009
Available online 10 March 2009

We have investigated the viscoelastic properties of the cytoplasmic intermediate filament (IF) proteins desmin and vimentin. Mechanical measurements were supported by time-dependent electron microscopy studies of the assembly process under similar conditions. Network formation starts within 2 min, but it takes more than 30 min until equilibrium mechanical network strength is reached. Filament bundling is more pronounced for desmin than for vimentin. Desmin filaments (persistence length $l_p \approx 900$ nm) are stiffer than vimentin filaments ($l_p \approx 400$ nm), but both IFs are much more flexible than microfilaments. The concentration dependence of the plateau modulus $G_0 \sim c^{\alpha}$ is much weaker than predicted theoretically for networks of semiflexible filaments. This is more pronounced for vimentin ($\alpha = 0.47$) than for desmin ($\alpha = 0.70$). Both networks exhibit strain stiffening at large shear deformations. At the transition from linear to nonlinear viscoelastic response, only desmin shows characteristics of nonaffine network deformation. Strain stiffening and the maximum modulus occur at strain amplitudes about an order of magnitude larger than those for microfilaments. This is probably attributable to axial slippage within the tetramer building blocks of the IFs. Network deformation beyond a critical strain γ_{max} results in irreversible damage. Strain stiffening sets in at lower concentrations, is more pronounced, and is less sensitive to ionic strength for desmin than for vimentin. Hence, desmin exhibits strain stiffening even at low-salt concentrations, which is not observed for vimentin, and we conclude that the strength of electrostatic repulsion compared to the strength of attractive interactions forming the network junctions is significantly weaker for desmin than for vimentin filaments. These findings indicate that both IFs exhibit distinct mechanical properties that are adapted to their respective cellular surroundings [i.e., myocytes (desmin) and fibroblasts (vimentin)].

Keywords: desmin and vimentin intermediate filament; electron microscopy; rheology; persistence length; strain stiffening

Edited by M. Moody

Introduction

The form and shape of metazoan cells are established by the coordinated function of three distinct filamentous systems, namely, microtubules, microfilaments (F-actin), and intermediate filaments (IFs). The individual filaments of the three groups are integrated by associated proteins—including cross-bridging factors of the plakin family, as well as motor protein complexes—and thereby constitute cell-type-specific three-dimensional networks.[1] These so-called cytoskeletons are by no means static structures, as they can be remodeled rapidly. In addition, individual cells are subjected to considerable forces depending on their tissue context. Hence,

*Corresponding author. E-mail address: norbert.willenbacher@mvm.uni-karlsruhe.de.

† M.S. and H.B. contributed equally to this work.

Abbreviations used: IF, intermediate filament; LS, low salt; HS, high salt.

the existence of optimized mechanisms to resist mechanical stress is of prime importance during various cellular activities such as cellular locomotion, cell division, and intracellular trafficking.[2,3]

Tissue-forming metazoans express complex patterns of distinct IF proteins following certain routes of embryonic development.[4] This cell-type-specific expression program indicates that their networks exhibit distinct properties optimized for their respective cellular functions. Myocytes, in particular, have to endure substantial external and internal mechanical forces. The muscle-specific IF protein desmin, in concert with synemin, plectin, and other desmin-binding factors, forms an extrasarcomeric filamentous network that helps to coordinate mechanical interaction between neighboring cells and working sarcomeric units within individual cells. Moreover, desmin IFs are likely to be involved in mechanosensing and mechanotransduction processes.[5,6] During the development of mammalian skeletal[7] and cardiac muscle cells,[8] vimentin is expressed first and later on replaced gradually by desmin, which is then persistently expressed in adult muscle fibers.[4,9] Desmin filaments link the contractile apparatus to myotendinous junctions and the Z-line structure of skeletal muscles, as well as to desmosomes of intercalated disks of cardiac muscles. In addition, desmin IFs directly connect to complexes presented by the outer membranes of the nuclear envelope.[10] They furthermore provide a connection to organelles such as mitochondria and lysosomes and support associated proteins such as αB-crystallin and plectin.[5,11] The rationale underlying the replacement of vimentin by desmin during the development of mature muscle fibers is not known. Although both vimentin and desmin exhibit a high degree of sequence similarity[12,13] and are able to copolymerize at all stages of filament assembly,[14] their properties differ significantly. Under standard assembly conditions, desmin forms filaments with a higher number of subunits per cross-section and assembles much faster than vimentin.[14,15] Moreover, desmin filaments exhibit a higher tendency to associate with each other compared to vimentin IFs, as has been determined by electron microscopy and capillary viscosity measurements.[16] Hence, desmin IFs display distinct biophysical properties that might reflect the optimization process that occurred during evolution to facilitate proper muscle function.

More than 40 human diseases arising from mutations in IF genes, among them skeletal and cardiac myopathies caused by mutations in the desmin gene, have been characterized.[17] Their severity calls for a better understanding of the role that IFs play in normal cellular function. Therefore, the specific biophysical features of IF networks are of fundamental interest. Up to now, the mechanical properties have mainly been studied for microfilaments and microtubules.[18–21] However, in one fundamental study, the mechanical properties of microtubules, microfilaments, and vimentin IFs have been directly compared by torsion pendulum rheometry.[22] Here, the authors demonstrate that IFs exhibit a very pronounced increase in their elastic modulus or "stiffness" upon increases in shear stress—a phenomenon specified as "strain hardening" or "strain stiffening." Following this report, several IF proteins, including keratins, vimentin, and neurofilament proteins, were investigated in more detail.[22–27]

Here we report for the first time on the viscoelastic properties of *in-vitro*-assembled desmin filament networks as measured by mechanical rheometry. From the linear viscoelastic response in different frequency regimes, we have deduced the mesh size ξ of the networks (the mean distance between two network junctions) and the persistence length l_p of individual filaments, which is directly related to the bending stiffness $\kappa = k_B T l_p$. Furthermore, we have characterized network deformation and rupture using nonlinear oscillatory shear. The properties of pure desmin IFs have been compared with those of vimentin IFs, as well as with those of heteropolymeric IFs coassembled from both proteins.

Results and Discussion

Electron microscopy of desmin and vimentin network formation

The specific viscoelastic properties of molecularly distinct biopolymer gels depend critically on the detailed assembly and geometry of the observed material. For assembly studies of desmin and vimentin by transmission electron microscopy and capillary viscometry, protein concentrations of 0.1–0.5 g/l and salt concentrations of 50–160 mM NaCl have routinely been employed.[28–31] These conditions define a meaningful physiological range, where single extended IFs are usually visualized in fixed and negatively stained samples. However, the aforementioned protein concentrations were found to be far too low for the rheological studies performed here. Thus, the experiments were performed at higher concentrations of around 1.0 g/l to obtain reproducible data. So far, electron microscopic analysis has not been performed for these concentrations. Therefore, we have investigated the time-dependent assembly process of desmin and vimentin at 1.0 g/l in the presence of 50 mM sodium chloride ["low salt" (LS)]. After careful dilution of the samples to 0.1 g/l with glutaraldehyde-containing "assembly buffer," filaments and networks were observed to be evenly distributed on the grids upon electron microscopy. Characteristic images taken at different stages of assembly are shown in Fig. 1. After 10 s, most of the unit length filaments have already been consumed by longitudinal annealing and have formed filaments of up to 600 nm long. Notably, lateral association of unit length filaments and short filaments is entirely absent at initial time points (10 s; left). After 2 min, extensive filament elongation and lateral association of individual filaments have resulted in the formation of complex networks (middle). After 7.5 min, filaments show

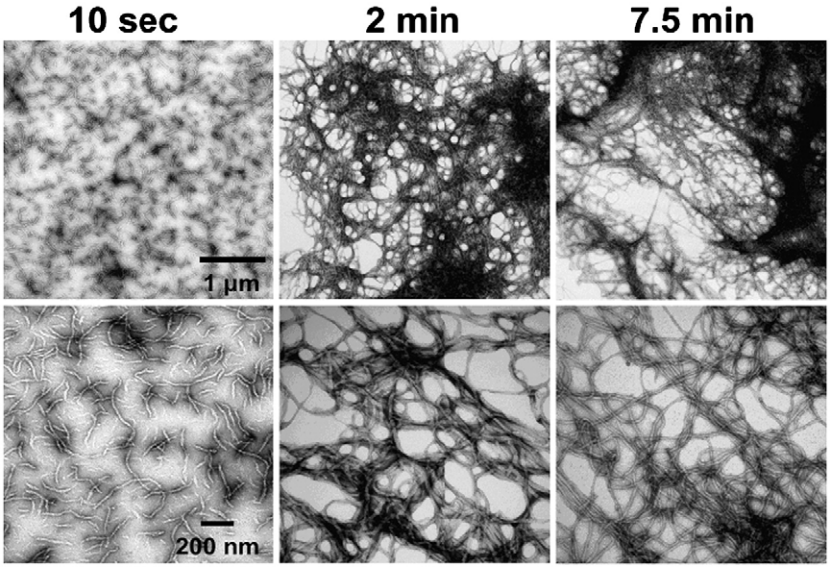

Fig. 1. Electron microscopic analysis of negatively stained early assembly intermediates of desmin. Assembly was performed at 1.0 g/l under LS conditions for 10 s, 2 min and 7.5 min. Upper panels: Overview of network formation. Lower panels: Detailed view showing single IFs loosely associating filaments that, on occasion, run in parallel for limited distances. Scale bars represent 1 μm (upper panels) and 200 nm (lower panels).

considerable radial compaction (right). The degree of bundling of individual filaments is comparable to that observed after 2 min; however, some individual filaments are also discernable, indicating that lateral association of filaments is reduced after radial compaction has occurred. Next, we compare electron micrographs for filament and network formation at physiological salt concentration [i.e., 160 mM sodium chloride; "high salt" (HS)] with those under LS conditions for both desmin and vimentin (Fig. 2). Both proteins form smooth, extended *bona fide* IFs upon addition of "assembly buffer," as depicted here for filaments assembled for 30 min. Notably, vimentin does not form significant bundles of filaments under LS conditions (Fig. 2a). These results already indicate that, in comparison to vimentin, the ratio of repulsive to attractive electrostatic interactions forming network junctions is significantly weaker for desmin. Moreover, the filaments obtained are considerably thicker under HS assembly conditions than under LS assembly conditions: the filament diameter for vimentin is measured to be 11.7±1.3 nm (HS) *versus* 9.7±1.4 nm (LS; Fig. 2b and a); for desmin, the corresponding values obtained are 13.1±1.8 nm (HS) *versus* 12.2±1.8 nm (LS; Fig. 2d and c). The diameter of an IF is a direct indicator of filament mass, as has been demonstrated previously by scanning transmission electron microscopy measurements.[15,29] If and how this may influence the viscoelastic properties of the IFs were approached by the following rheometric investigations.

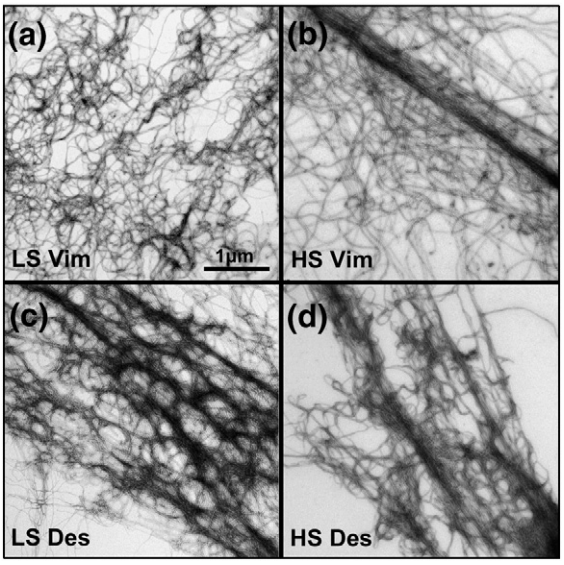

Fig. 2. Mature IF networks obtained from (a and b) vimentin and (c and d) desmin under (a and c) LS and (b and d) HS conditions, respectively, after 30 min of assembly. Scale bar represents 1 μm.

The storage modulus of desmin and vimentin IFs

In a first set of experiments, we determined the storage modulus (G') of desmin and vimentin solutions under LS and HS conditions. The time-dependent evolution of the storage modulus during assembly exhibited a distinct behavior for desmin under HS conditions: the increase in G' is slightly slower, and the final value is almost half compared to the other samples (Fig. 3, black squares). In contrast, desmin under LS conditions (open squares) and vimentin at both salt concentrations (circles) exhibited a similar increase in G' and the same final value for the storage modulus. In either case, the first steep increase correlates with a very fast network formation, as also seen in electron micrographs. Obviously, filament assembly and network formation occur simultaneously, but it takes 30–60 min until a "mature" network architecture with its equilibrium mechanical properties is formed. This correlates to the late phase of compaction and may arise from changes in surface properties and in the flexibility of individual filaments.[30,32] Hence, our oscillatory shear data facilitate a novel in-depth insight into the

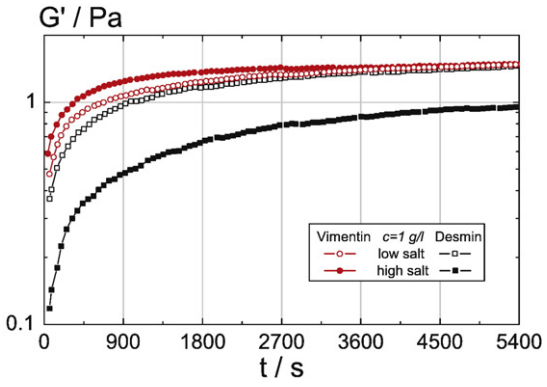

Fig. 3. Storage modulus G' during the filament assembly of desmin (square) and vimentin (circle) at a protein concentration $c=1.0$ g/l and 37 °C. Assembled under LS (open symbols) and HS (closed symbols) conditions.

subtleties of the filament maturation phase, which was previously not detectable by electron microscopy and atomic force microscopy.[14,33,34] The lower final value of G' for desmin polymerized under HS conditions may be rationalized in terms of the larger filament diameter and the stronger bundling, as revealed by electron microscopy. Finally, as at least 80% of the final G' level is reached within 30 min of assembly initiation, we have chosen this period of time for protein assembly and network formation prior to the rheological measurements presented below.

Linear viscoelastic filament and network response: Persistence length of filaments

We employed high-frequency oscillatory shear experiments in order to determine the bending stiffness of desmin and vimentin IFs assembled under LS conditions. Semiflexible objects such as IFs exhibit a distinct scaling behavior for the frequency dependence of the linear viscoelastic shear modulus $G^*=G'+iG''$. In the frequency regime where internal relaxation modes of individual Kuhn segments dominate, $G^*\sim\omega^{3/4}$ holds,[35] and the absolute value of G^* is related to the persistence length l_p, therefore characterizing the flexibility of the filament chain:[36]

$$G^* - i\omega\eta_s = \frac{1}{15}\rho\kappa l_p\left(\frac{-2i\zeta}{\kappa}\right)^{3/4}\omega^{3/4} \qquad (1)$$

where η_s is the solvent viscosity (here, water at 37 °C), $\kappa=k_BTl_p$ is the bending modulus, ζ is the lateral drag coefficient, and ρ is the area density of the filaments. We insert $\zeta=4\pi\eta_s/\ln(0.6\lambda/d_f)$ for the lateral drag coefficient, with d_f as the diameter of the mature filaments. For the characteristic length scale λ, we choose the mesh size ξ of the network, which is calculated from the plateau modulus G_0 according to $\xi=\sqrt[3]{kT/G_0}$. The latter is defined as the linear viscoelastic modulus G' of the network in the regime, where G' is independent of frequency. The onset of this $\omega^{3/4}$ scaling is related to the highest Zimm relaxation frequency $\omega_0=k_BT/8\eta_s l_p^3$, which can also be used to obtain the persistence length l_p. This concept has been successfully used to determine l_p for solutions of worm-like micelles[37] representing another class of self-assembling semiflexible objects. The occurrence of $G\sim\omega^{3/4}$ has also been observed for F-actin solutions.[38,39]

Figure 4 shows the frequency dependence of the reduced loss modulus $(G''-\omega\eta_s)/c$ for desmin (LS) solutions at protein concentrations between 1.0 g/l and 2.8 g/l. The moduli are divided by concentration, since linear concentration dependence is expected in the frequency range where internal relaxations of individual Kuhn segments dominate. The data superimpose nicely in the frequency range where the $\omega^{3/4}$ scaling is valid. From these data, the persistence length of human wild-type desmin is determined according to Eq. (1) as $l_p=685\pm65$ nm. The corresponding l_p values, as well as the physical parameters required to calculate l_p, are summarized in Table 1. There is no indication of a concentration-dependent structural change that would affect the bending stiffness of the desmin filaments. For the three lowest concentrations, the $\omega^{3/4}$ scaling is observed throughout the investigated frequency range from 10 s^{-1} to 10^4 s^{-1}. For $c=2.8$ g/l, the reduced loss modulus starts to deviate substantially from the other data especially at lower frequencies, and the $\omega^{3/4}$ scaling is found only for frequencies $\omega>1000$ rad/s. At lower frequencies, the characteristic Zimm scaling $G^*\sim\omega^{5/9}$ is found. The l_p value determined from the highest Zimm relaxation frequency $\omega_0\approx1000$ rad/s (cross-over from $\omega^{5/9}$ to $\omega^{3/4}$ scaling) is $l_p=350$ nm; on the other hand, application of Eq. (1) yields $l_p=754$ nm. This discrepancy indicates that, at this high concentration, the Zimm model may not be applicable, and the apparent relaxation time ω_0 is not suitable for the determination of l_p.

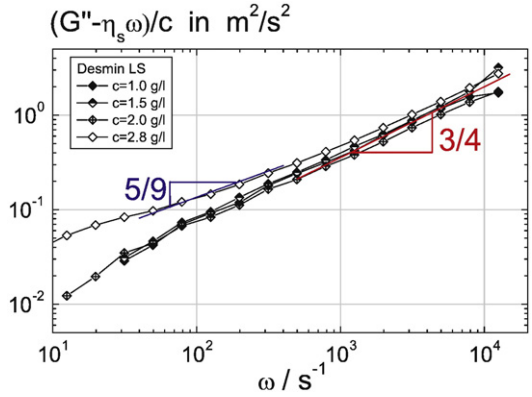

Fig. 4. Concentration dependence of the reduced linear viscoelastic loss modulus G'' of desmin (LS), as determined from oscillatory squeeze flow measurements. G'' varies linearly with concentration in the frequency range investigated here up to $c=2.0$ g/l. Thus, these data allow for the determination of the persistence length l_p according to Eq. (1).

Table 1. Plateau moduli, mesh sizes, and persistence lengths of desmin (LS) and vimentin (HS)

Desmin (LS)					Vimentin (HS)		
c (g/l)	G_0 (Pa)	ξ (nm)	ζ (Ns/m²)	l_p (nm)	c (g/l)	G_0 (Pa)	ξ (nm)
0.4	0.19	280			0.5	0.60	190
0.5	0.5	205			1.0	0.78	175
0.7	0.55	200			1.5	0.89	170
1.0	0.6	195	0.0039	691	2.0	1.23	150
1.4	0.95	165	0.0042	699			
2.0	1.0	160	0.0043	597			
2.8	1.8	135	0.0046	754			

In another set of experiments, we have determined the persistence lengths of desmin, vimentin, and a 1:1 (by weight) mixture of both proteins under LS conditions from G'' measurements at a single concentration $c=1.0$ g/l. All values are summarized in Table 2. Obviously, desmin filaments are substantially stiffer than vimentin filaments, and the l_p of the former is about twice as high as that of the latter. This confirms electron microscopy results revealing a larger filament diameter and stronger bundling for desmin compared to vimentin especially under LS conditions. The stiffness of the mixed filaments lies between that of the individual filaments.

It has to be noted that the l_p value for desmin (in the latter experiment, $l_p=895\pm50$ nm) differs far more from the former experiment than the statistical range of error inferred from the analysis of a series of experiments performed on filament solutions assembled from a single batch. This points to the inherent polymorphism of desmin filament assembly.

The l_p value for human wild-type vimentin obtained here ($l_p=415\pm45$ nm) agrees very well with data reported earlier, where l_p was deduced from the contour analysis of single vimentin filaments adsorbed to solid substrates as imaged by atomic force microscopy.[40] In this study, an l_p value of about 1000 nm was obtained. Taking into account the different experimental approaches and batch-to-batch variations of the protein solutions, this is considered to be in good agreement with the results reported here. Our data also agree well with an earlier estimate of $l_p\approx100$–1000 nm for desmin purified from chicken gizzard, which was based on dynamic light-scattering results.[41]

Finally, it is out of doubt that desmin and vimentin IFs are much more flexible than microfilaments for which l_p values between 3 μm and 18 μm have been reported.[42–46]

Table 2. Filament diameters, mesh sizes, and persistence lengths of desmin, vimentin, and their mixture

Proteins[a]	d_f (nm)	ξ (nm)	ζ (Ns/m²)	l_p (nm)
Desmin	12.2±1.8	195±7	0.0039±0.0002	895±50
Vimentin	9.7±1.4	195±7	0.0035±0.0002	415±45
Desmin+Vimentin[b]	11.0±1.6	195±6	0.0037±0.0002	715±55

[a] Assembly was carried out at 1.0 g/l under LS conditions.
[b] Both proteins were mixed in 8 M urea prior to renaturation.

At a first glance, this is surprising, since F-actin has a smaller outer diameter (≈7–8 nm) and an even lower mass per length (16 kDa/nm) than desmin (48±8 kDa/nm) or vimentin (33±4 kDa/nm).[14,30] This might be attributed to an intrafilamentous axial slippage of distinct building blocks, which can occur without disrupting the molecular architecture, whereas the two strands forming the microfilament are tightly bonded together.[40,47]

Mesh size of filament networks

Polymer networks exhibit a characteristic frequency range where G' is much larger than G'' and independent of frequency. The corresponding value of G' is called plateau modulus G_0; within the framework of classical entropy (rubber) elasticity,[48] this quantity is directly proportional to the cross-link density ν of the network $G_0=\nu k_BT$. Figure 5 shows the concentration dependence of G_0 for vimentin and desmin. In both cases, a power law behavior $G_0\sim c_p^{\alpha}$ is observed, with $\alpha=0.70\pm0.17$ for desmin and $\alpha=0.47\pm0.1$ for vimentin. For the latter, our value for the exponent α is in very good agreement with earlier results.[22] For both vimentin and desmin IFs, α is significantly lower than those for other protein filaments such as fibrin ($\alpha\approx2.2$) or for microtubules and neurofilaments ($\alpha\approx1.3$). For microfilaments assembled with different amounts of bivalent ions or cross-linkers, values of $\alpha=2.2$[22] and $\alpha=1.4$,[39] respectively, have been reported.

Moreover, the exponents measured here lie far below the theoretical value of $\alpha=7/5$[49,50] derived for entangled networks of semiflexible chains with $l_p\gg\xi$, which is fulfilled here (see Table 1), and deviate even more from the theoretical prediction for the affine deformation of cross-linked networks for which a value of $\alpha=11/5$ is expected.[51]

Assuming a homogeneous entropy elastic network, G_0 can be directly related to the mesh size of that network via $\xi=\sqrt[3]{kT/G_0}$. The corresponding ξ values for desmin and vimentin are summarized in

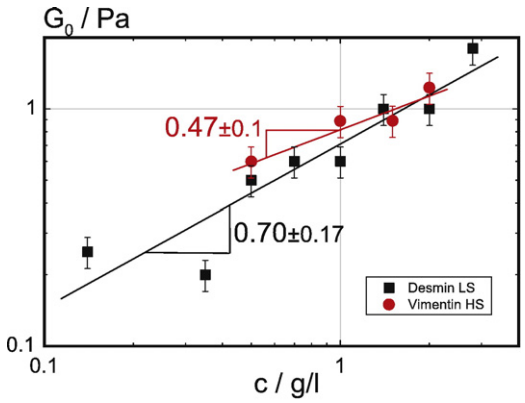

Fig. 5. Concentration dependence of the linear viscoelastic storage modulus G_0 for desmin (LS) concentrations of $0.1<c<2.8$ g/l (squares) and vimentin (HS) concentrations of $0.5<c<2.0$ g/l. In this concentration range, the storage modulus follows power laws of $G'\sim c^{0.7}$ for desmin and $G'\sim c^{0.5}$ for vimentin.

Table 1. The mesh size decreases with increasing concentration according to $\xi \sim c^{-\beta}$. For desmin and vimentin, $\beta = 0.25 \pm 0.1$ and $\beta = 0.15 \pm 0.1$ are found, respectively, due to the weak dependence of G_0 on concentration. A significantly stronger variation of mesh size with concentration has been reported for actin filaments ($\beta = 0.5$)[52] and neurofilaments ($\beta = 0.44$).[26] At this point, we would like to mention that the mesh size in these latter cases has been determined from the Brownian motion of tracer particles. In the case of actin, the ξ values one can calculate from G_0 data,[53] as described above, agree very well with those from microrheology, whereas in the case of neurofilaments, the mesh size according to tracer particle motion is, by far, larger than expected from the corresponding G_0 data. For desmin and vimentin, no microrheological data are available so far, and an in-depth discussion of this topic is outside the scope of this work.

The low α and β values for desmin or vimentin suggest that the filament structure does not remain constant as concentration is varied. The electron micrographs taken at a concentration of 1 g/l (Fig. 2) show significant bundling of desmin filaments, while the vimentin network is essentially built by single filaments. Therefore, it seems reasonable to attribute the weak concentration dependence of the modulus G_0 in the case of desmin to an increase in bundling with increasing concentration. For vimentin, the formation of more and more short filaments not incorporated into the network could be a reasonable scenario, but since our electron microscopy data do not give evidence for the formation of a significant fraction of such short filaments, we may leave this as a yet unspecified structural property of vimentin networks.

Nonlinear filament network deformation and rupture

Figure 6 plots the storage modulus G' as a function of strain amplitude at fixed angular frequency $\omega = 1$ rad/s for five different protein filament networks, namely, desmin and vimentin under LS and HS conditions, as well as an equimolar mixture of both proteins under LS conditions only. In all cases, the protein concentration c is kept constant at 1.0 g/l. All samples exhibit linear viscoelastic behavior at low strain amplitudes (i.e., G' is independent of γ). The absolute values of G' are essentially the same for all samples and lie in the range of $0.5 < G' < 0.8$ Pa. The onset of nonlinear response is observed at strain amplitudes of $0.25 < \gamma_c < 0.35$. For vimentin at LS concentration, the storage modulus decreases monotonically with increasing strain amplitude, while for all other samples, G' shows strain stiffening and exhibits a maximum at strain amplitudes of $1.5 < \gamma_{max} < 5$. Finally, G' decreases when the sample breaks and the upper cone of the rheometer loses contact with the filament network. The behavior of the desmin–vimentin mixture lies between that of the pure solutions of these proteins and exhibits weak strain stiffening. For desmin at HS concentration, the maximum value of the storage modulus G_{max} exceeds the linear viscoelastic value $G_0 = lim_{\gamma \to 0} G'$ by a factor of 5. Corresponding values at different protein and salt concentrations for desmin and vimentin have been summarized in Table 3.

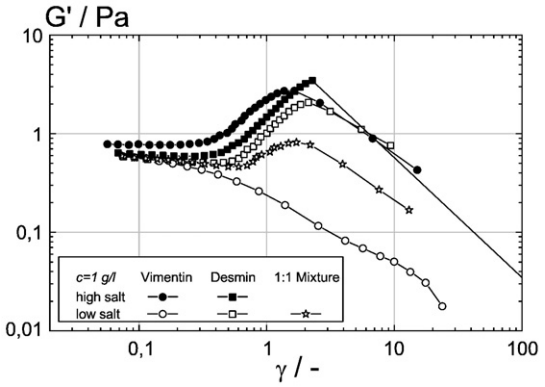

Fig. 6. The storage modulus G' for desmin (square) and vimentin (circle) networks at a protein concentration of $c = 1.0$ g/l depends on salt concentration. The assembly was performed under LS (open symbols) and HS (closed symbols) conditions, respectively. A 1:1 mixture of vimentin and desmin coassembles and shows a behavior between the pure protein solutions.

Figure 7 shows the strain amplitude dependence of G' for protein solutions at different concentrations. Figure 7a shows the behavior of desmin under LS conditions, whereas Fig. 7b depicts the data measured for vimentin under HS conditions. Desmin solutions exhibit strain stiffening at protein concentrations $c \geq 0.4$ g/l even under LS conditions, while vimentin does not show strain stiffening under LS conditions in the concentration range investigated here ($c \leq 1.0$ g/l), but it is known to show strain stiffening at much higher concentrations ($c = 2.0$ g/l) and under buffer conditions with much higher ionic strength.[22] Under HS conditions, vimentin exhibits strain stiffening already at concentrations above $c = 0.5$ g/l. For both proteins, the degree of strain stiffening increases with increasing protein concentration. At similar concentrations, however, strain stiffening is more pronounced for desmin (even under LS conditions) than for vimentin. In accordance with the weaker concentration dependence of G_0, we attribute this to the stronger tendency for bundling and/or formation of short filament sequences in the case of vimentin. Another difference in the two IF proteins (i.e., vimentin and desmin) becomes obvious upon closer inspection of the transition from linear to nonlinear viscoelastic response, as shown in Fig. 8. G' increases monotonically with γ, in agreement with previous results reported for vimentin but also similar to those known for actin, fibrin, collagen, and neurofilaments.[27] In contrast, G' goes through a minimum before strain stiffening sets in for desmin. This might indicate nonaffine network deformation, as suggested previously by finite-element analysis

Table 3. Plateau and maximum storage moduli and their ratios

Desmin (LS)			Vimentin (HS)		
c (g/l)	G_0 (Pa)	G_{max}/G_0	c (g/l)	G_0 (Pa)	G_{max}/G_0
0.4	0.19	1.4	1.0	0.78	3.5
0.7	0.55	3.8	1.5	0.89	3.8
1.0	0.56	3.6	2.0	1.23	4.4
1.4	0.95	7.6			

of a two-dimensional network model.[54] This phenomenon is observed under HS and LS conditions for concentrations of 1 g/l and below, but G' exhibits a monotonic increase for $c=1.4$ g/l.

The dependence of G' and G'' on deformation amplitude for three subsequent measurements performed on a desmin solution (LS) with $c=1.0$ g/l is shown in Fig. 9. The first set of data acquisition is stopped before the maximum value of G' (or G'', respectively) is reached. Under these conditions, the deformation of the network is completely reversible. The second evaluation yields exactly the same

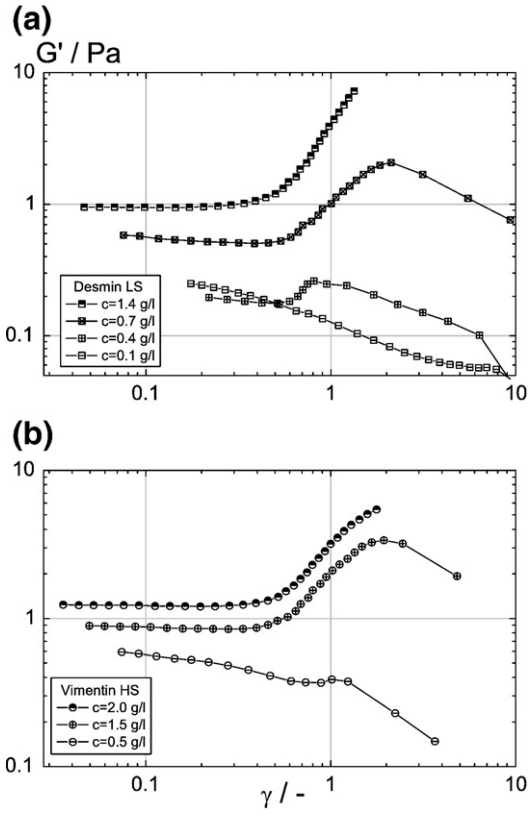

Fig. 7. (a) Concentration dependence of the storage modulus G' for desmin networks under LS conditions (lined square, 0.1 g/l; uprightly crossed square, 0.4 g/l; diagonally crossed square, 0.7 g/l; half-filled square, 1.4 g/l). Note that, below a concentration of $c\approx0.4$ g/l, no strain stiffening occurs. For all other concentrations examined, strain stiffening starts at a critical strain of $\gamma_c\approx0.5$. (b) Concentration dependence of the storage modulus G' for vimentin networks under HS conditions. Again, strain stiffening sets in at $\gamma_c\approx0.5$ for vimentin concentrations above 0.5 g/l.

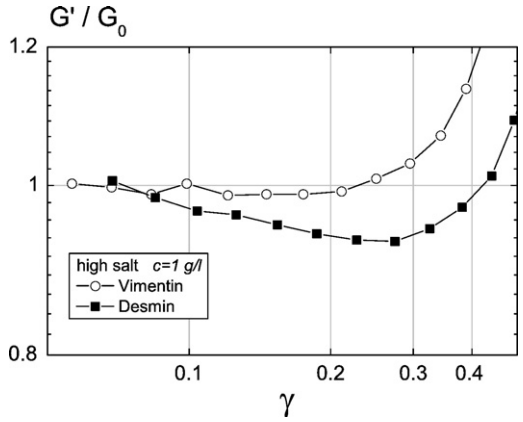

Fig. 8. Storage modulus G' *versus* shear strain amplitude γ at the transition from linear response to nonlinear response.

G',G'' values as obtained for the first one, also indicating that the assembly time of 1800 s, which we chose as a starting point for our experiments, is sufficient. In the second run, γ is increased until rupture of the network solution occurs, leading to irreversible damage of the network structure. The third evaluation of the sample performed after a recovery time of 10 min yields a significantly lower value of G_0, and less pronounced strain stiffening is observed.

Strain stiffening is a well-known phenomenon for cross-linked semiflexible protein filament networks and has been reported for F-actin,[18,22] neurofilaments,[26,27] collagen, and fibrin,[27] as well as for keratin[24] and vimentin.[22] It is widely accepted that this strain stiffening is partly entropic and

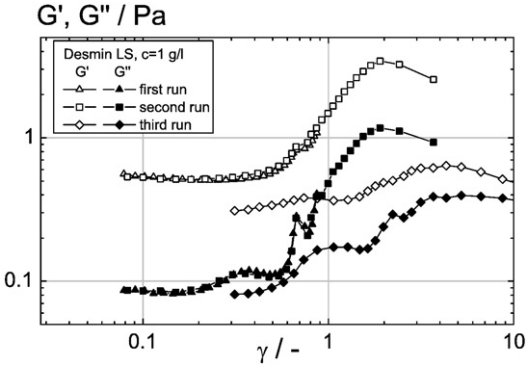

Fig. 9. Deformation dependence of storage modulus G' and loss modulus G'' for a desmin solution (LS) with $c=1.0$ g/l. The moduli are shown for three subsequent measurements on the same sample. In the first run (triangles), the maximum strain amplitude was chosen such that the maximum in G' was not yet reached. In the second run (squares), γ was increased until rupture of the sample occurred, and the third run was performed after a recovery time of 10 min. Note the exact reproducibility of the G' and G'' values obtained for low strains. Beyond a critical stress, however, the sample fails and will not recover its capability to exhibit strain stiffening even after prolonged periods of rest (up to 40 min; data not shown).

partly enthalpic in nature, in particular when the persistence length is of the same order of magnitude or even larger than the mesh size ($l_p \geq \xi$). Stretching the network results in a loss of thermally accessible conformations of the semiflexible filament strands between two cross-links, leading to a strong increase in entropic stress. On the other hand, network deformation results in bending, buckling, and elongation of filaments, increasing enthalpic stresses. The onset of strain stiffening is dominated by entropic effects, while enthalpic effects progressively contribute at higher γ.[27] Accordingly, statistical mechanical models have been developed to describe these phenomena. The glassy worm-like chain model[55] is a phenomenological extension of the single filament worm-like chain model. The effect of the network junctions apparently results in a strong exponential stretching of the stress relaxation spectrum. The influence of various physicochemical interactions among filaments is represented by a single stretching parameter ε. Qualitatively, this model resembles the strain stiffening features observed for desmin and vimentin. A quantitative comparison would require numerical simulations that are beyond the scope of this work. Recently published results for F-actin[20] refer to the differential modulus K^*, which is different from the G^* data presented here. Storm *et al.* started with the stress–strain curve of an individual filament and assumed affine deformation of a homogenous isotropic network.[27] Finite longitudinal compliance of the filaments has to be considered in order to recover the increase in the differential shear modulus observed for vimentin, actin, fibrin, and collagen, which is much less pronounced than expected for a purely entropic stress response.

The shape of G' *versus* γ at intermediate strains seems to be generic for all semiflexible systems, including vimentin.[27] We cannot directly compare the shape of the curves presented here to those in literature data, since we have not measured the differential modulus. But the shapes of the modulus *versus* strain curves in the strain stiffening regime look quite similar for both desmin and vimentin, and we conclude that desmin shows the same generic strain stiffening behavior as the other protein filament networks, except for the slight depression of the G'–γ curves before stiffening sets in. Nevertheless, the protein concentration required for network formation, the maximum degree of strain stiffening, and the strain at which the network ruptures strongly depend on the molecular structure determining filament extensibility and, above all, on the nature and strength of the physicochemical bonds holding the filaments together. Apparently, in contrast to vimentin, a much lower protein concentration is required for desmin in order to form a mature network.

This might be again due to the stronger tendency for bundling of desmin and the formation of shorter filaments in the case of vimentin.

Furthermore, desmin is less sensitive to ionic strength and shows strain stiffening even under LS conditions. This can be rationalized by a competition between short-range attractive van der Waals and hydrophobic interactions *versus* long-range electrostatic repulsion among filaments. In case of vimentin (LS), electrostatic repulsion is strong enough to prevent cross-linking and network formation. Thus, for vimentin, strain stiffening can take place only at HS concentrations, when the range of electrostatic repulsion is shorter, or at high protein concentrations, when the filaments are more densely packed.

Desmin shows pronounced strain stiffening even at LS concentration, indicating that electrostatic repulsion is weaker and not able to prevent the formation of cross-links promoted by attractive interactions. At similar protein and salt concentrations, but also at similar linear viscoelastic moduli, the G_{max}/G_0 ratio is significantly larger for desmin than for vimentin. This indicates a higher bond strength for desmin networks than for vimentin networks. We have investigated the reversibility of the nonlinear network deformation for desmin (LS). As long as $\gamma < \gamma_{max}$ is valid, strain stiffening is perfectly reversible. However, as soon as the critical deformation γ_{max} is exceeded and the network ruptures, filament networks are irreversibly damaged, and the original strain stiffening properties cannot be regained even upon allowing longer interval periods between successive measurements (up to 1 h; data not shown). This is similar to what has been reported for cross-linked F-actin,[18] but γ_{max} is almost an order of magnitude larger for both desmin and vimentin compared to F-actin, which might also be a consequence of the axial slippage allowed between subfilamentous elements such as tetrameric or octameric complexes within the IF.

Conclusion

We have investigated the linear and nonlinear viscoelastic properties of desmin and compared them to those of vimentin filament networks. The persistence length l_p of the filaments has been derived from the linear viscoelastic modulus in the high-frequency range where $G^* \sim \omega^{3/4}$. Desmin is stiffer than vimentin ($l_p^{desmin} \approx 900$ nm; $l_p^{vimentin} \approx 400$ nm under LS conditions), but both IFs are much more flexible than microfilaments. A mesh size $\xi \approx 200$ nm is obtained from the low-frequency plateau modulus G_0 in the concentration range $0.5 < c < 2$ g/l in both cases.

The concentration dependence of $G_0 \sim c^{\alpha}$ is much weaker than those predicted by theoretical models for networks of semiflexible filaments. For desmin ($\alpha = 0.70$), this may be explained by increased bundling with increasing protein concentration; for vimentin ($\alpha = 0.47$), the structural reason is not yet clear. In contrast, microfilament or neurofilament networks do not show this phenomenon. Both desmin and vimentin networks exhibit pronounced strain stiffening at large shear deformations similar to those of many other protein filament networks.

At the transition from linear to nonlinear viscoelastic response, the desmin network exhibits a minimum in G', which is characteristic of nonaffine network deformation, whereas G' increases monotonically in the vimentin case. Strain stiffening is controlled by enthalpic and entropic effects as expected, since $l_p > \xi$. The onset of strain stiffening occurs around $\gamma_c \approx 0.3$, and the modulus goes through a maximum at $\gamma_{max} = 1.5–5$. These values are about an order of magnitude larger than the γ_{max} values reported for F-actin and are again attributed to the axial slippage within building blocks of individual IFs. Deformation of the desmin network beyond γ_{max} results in an irreversible damage, and the original elastic properties are not recovered even upon extending the time interval to 1 h. Strain stiffening sets in at lower concentrations and—at a similar concentration—is more pronounced for desmin than for vimentin. Furthermore, strain stiffening is less sensitive to the ionic strength of the solution for desmin compared to vimentin networks, and the desmin networks exhibit strain stiffening even at LS concentrations. These results clearly indicate that the strength of repulsive electrostatic interactions compared to the strength of attractive interactions forming the network junctions is significantly weaker for desmin than for vimentin filaments. Finally, we found that heteropolymeric filaments assembled from both desmin and vimentin exhibit features in between those of the individual proteins. This is true for the filament persistence length l_p, as well as for the strain stiffening properties of the networks.

Future experiments are aimed at elucidating how posttranslational modifications such as phosphorylation, as well as interaction with IF-associated proteins, influence the viscoelastic properties of desmin and vimentin networks. By increasing the degree of complexity in the constitution of the analyzed networks, we ultimately hope to get a basic insight into the nanomechanics of the extrasarcomeric cytoskeleton of myocytes and fibroblasts. In addition, the rheological analysis of disease-causing mutant desmin filaments could provide an insight into the molecular mechanisms underlying a severe form of (cardio)myopathy in humans. As desmin IFs are thought to be involved in mechanosensing and mechanotransduction in muscle tissues, alterations in biophysical filament and network properties due to mutations are likely to impact on these fundamental properties.

Materials and Methods

Protein chemical methods

Escherichia coli strain TG1 (Amersham, Germany) was transformed with human wild-type desmin and vimentin plasmids, respectively. Recombinant proteins were purified from inclusion bodies, as described previously.[28,56] For *in vitro* reconstitution of purified recombinant proteins, up to 4.0 g/l protein was dialyzed out of 8 M urea and 10 mM Tris–HCl (pH 7.5) into a buffer containing 5 mM Tris–HCl (pH 8.4), 1 mM ethylenediaminetetraacetic acid, 0.1 mM ethylene glycol bis(*b*-aminoethyl ether) *N*, *N*′-tetraacetic acid, and 1 mM DTT ("Tris buffer") using regenerated cellulose dialysis tubing (Spectra/Por®; molecular weight cutoff, 50,000; Roth, Germany). For assembly experiments, protein solutions were heated to 37 °C, and assembly was initiated by addition of an equal volume of either LS [45 mM Tris–HCl (pH 7.0) and 100 mM NaCl] or HS [45 mM Tris–HCl (pH 7.0) and 320 mM NaCl] "assembly buffer." For mixing experiments, equimolar amounts of desmin and vimentin proteins were combined in 9.5 M urea prior to dialysis into "Tris buffer" in order to allow heterocomplex formation.

For all rheological measurements, protein solutions were filled into the preheated sample cell directly after initiation of assembly, and gap height was immediately set. Then a waiting time of 30 min was allowed for the assembly of the filaments to occur before the measurements were started, except for the experiments in which the kinetics of filament network formation were characterized.

Electron microscopy

After assembly at 1.0 g/l, the samples were diluted to a concentration of 0.1 g/l in fixation buffer prior to absorption to glow-discharged Formvar/carbon-coated copper grids and negative staining with a 15-s treatment with 0.1% uranyl acetate. The specimens were inspected, and micrographs were recorded on a Zeiss model 900 transmission electron microscope (Carl Zeiss, Oberkochen, Germany), as described previously.[29] Electron microscopic images were scanned and processed using the free software ImageJ 1.32j developed at the National Institutes of Health (Bethesda, MD, USA)‡. For filament width measurements, at least 100 filament diameters were determined.

Rheology

Low-frequency measurements

We used the commercial rheometers Haake RheoScope1 and Haake MARS II (Haake, Karlsruhe, Germany) to measure the storage modulus G' and the loss modulus G''. Both rheometers were equipped with cone and plate geometry with a cone angle of 4° and a truncation at the tip of 139 μm, corresponding to the set gap size. The sample volume counted 2 ml of protein solution, so the system was slightly overfilled. We conducted all measurements at a temperature of $T = 37$ °C. The lower measurement plate is flat with a diameter of 80 mm and tempered by a water cryostat. The upper part of the sample cell is built with a self-constructed heating plate. In this manner, the whole measurement configuration can be tempered homogeneously with a precision of ±0.02 °C.

In order to characterize the kinetics of filament assembly and network formation, we used small-amplitude oscillatory shear measurements and applied a strain $\gamma = \gamma_0 \sin\omega$ at a constant frequency of $\omega = 1$ rad/s and at a constant strain of $\gamma_0 = 0.05$ to ensure a linear viscoelastic response of the sample. The resulting stress signal $\tau = \tau_0 \sin(\omega + \delta)$ is also sinusoidal with a phase shift δ. $G' = (\tau_0/\gamma_0)\cos\delta$ and $G'' = (\tau_0/\gamma_0)\sin\delta$ were calculated from

‡ http://rsb.info.nih.gov/ij

the in-phase and out-of-phase components of τ. Data points were taken every 60 s starting immediately after filling the measuring device.

The nonlinear material response was characterized using stress amplitude sweep experiments. In this case, a sinusoidal stress $\tau = \tau_0 \sin(\omega)$ was applied, and the resulting strain $\gamma = \gamma_0 \sin(\omega + \delta)$ was measured. At a fixed frequency $\omega = 1$ rad/s, the stress amplitude τ_0 was varied between 10^{-2} Pa and 10 Pa (30 steps, logarithmically equidistant). At low stresses, the moduli G' and G'' are calculated from the in-phase and out-of-phase sinusoidal deformation signals, as described above. At larger deformations, the response signal differs from pure sinusoidal excitation. Then G' and G'' are calculated from the amplitude and the phase shift of the response signal in accordance with a company proprietary algorithm based on fast Fourier transform methods, including the third and fifth harmonics of the applied frequency.

High-frequency measurements

The characterization of the linear viscoelastic response of the protein suspensions was extended to frequencies beyond 100 rad/s using oscillatory squeeze flow via a piezo axial vibrator apparatus in accordance with published methods.[57,58] The sample is placed between two circular plates with a diameter of 20 mm and a distance of 10–30 μm, adjustable by different lids. The upper plate is constructed as a gas-tight lid and is tightly screwed to the base plate. The lower plate is driven through two pairs of piezoelectric actuators. By applying a sinusoidal voltage via a lock-in amplifier, the plate oscillates about a mean position. Two further piezoelectric sensor pairs deliver the response signal. We compared a measurement with sample with a measurement of the empty cell and calculated the desired rheological properties from the ratio of the output voltage with and without sample U/U_0 and the corresponding phase shift $\varphi - \varphi_0$. This device covers a frequency range from $10^1 < \omega < 5 \times 10^4$ rad/s and was tempered via a water cryostat.

Acknowledgements

H. Bär and H. Herrmann acknowledge grants from the German Research Foundation (DFG; grant BA 2186/2-1 to H.B., grant HE 1853 to H.H., and grant BA 2186/3-1 to H.B. and H.H.).

References

1. Herrmann, H., Bär, H., Kreplak, L., Strelkov, S. V. & Aebi, U. (2007). Intermediate filaments: from cell architecture to nanomechanics. *Nat. Rev. Mol. Cell Biol.* **8**, 562–573.
2. Kim, S. & Coulombe, P. A. (2007). Intermediate filament scaffolds fulfill mechanical, organizational, and signaling functions in the cytoplasm. *Genes Dev.* **21**, 1581–1597.
3. Toivola, D. M., Tao, G. Z., Habtezion, A., Liao, J. & Omary, M. B. (2005). Cellular integrity plus: organelle-related and protein-targeting functions of intermediate filaments. *Trends Cell Biol.* **15**, 608–617.
4. Lazarides, E. (1982). Intermediate filaments: a chemically heterogeneous, developmentally regulated class of proteins. *Annu. Rev. Biochem.* **51**, 219–250.
5. Bär, H., Strelkov, S. V., Sjoberg, G., Aebi, U. & Herrmann, H. (2004). The biology of desmin filaments: how do mutations affect their structure, assembly, and organization? *J. Struct. Biol.* **148**, 137–152.
6. Knöll, R., Hoshijima, M. & Chien, K. (2003). Cardiac mechanotransduction and implications for heart disease. *J. Mol. Med.* **81**, 750–756.
7. Sejersen, T. & Lendahl, U. (1993). Transient expression of the intermediate filament nestin during skeletal muscle development. *J. Cell Sci.* **106**, 1291–1300.
8. Kachinsky, A., Dominov, J. & Miller, J. (1995). Intermediate filaments in cardiac myogenesis: nestin in the developing mouse heart. *J. Histochem. Cytochem.* **43**, 843–847.
9. Quinlan, R. A. & Franke, W. W. (1982). Heteropolymer filaments of vimentin and desmin in vascular smooth muscle tissue and cultured baby hamster kidney cells demonstrated by chemical crosslinking. *Proc. Natl Acad. Sci. USA*, **79**, 3452–3456.
10. Capetanaki, Y. & Milner, D. J. (1998). Desmin cytoskeleton in muscle integrity and function. *Subcell. Biochem.* **31**, *463–495.*
11. Capetanaki, Y., Bloch Robert, J., Kouloumenta, A., Mavroidis, M. & Psarras, S. (2007). Muscle intermediate filaments and their links to membranes and membranous organelles. *Exp. Cell Res.* **313**, 2063–2076.
12. Fuchs, E. & Weber, K. (1994). Intermediate filaments: structure, dynamics, function, and disease. *Annu. Rev. Biochem.* **63**, 345–382.
13. Schaffeld, M., Herrmann, H., Schultess, J. & Markl, J. (2001). Vimentin and desmin of a cartilaginous fish, the shark *Scyliorhinus stellaris*: sequence, expression patterns and *in vitro* assembly. *Eur. J. Cell Biol.* **80**, 692–702.
14. Wickert, U., Mücke, N., Wedig, T., Müller, S. A., Aebi, U. & Herrmann, H. (2005). Characterization of the *in vitro* co-assembly process of the intermediate filament proteins vimentin and desmin: mixed polymers at all stages of assembly. *Eur. J. Cell Biol.* **84**, 379–391.
15. Herrmann, H., Häner, M., Brettel, M., Ku, N. O. & Aebi, U. (1999). Characterization of distinct early assembly units of different intermediate filament proteins. *J. Mol. Biol.* **286**, 1403–1420.
16. Bär, H., Mücke, N., Ringler, P., Müller, S. A., Kreplak, L., Katus, H. A. *et al.* (2006). Impact of disease mutations on the desmin filament assembly process. *J. Mol. Biol.* **360**, 1031–1042.
17. Omary, M. B., Coulombe, P. A. & McLean, W. H. I. (2004). Intermediate filament proteins and their associated diseases. *New Engl. J. Med.* **351**, 2087–2100.
18. Gardel, M. L., Shin, J. H., MacKintosh, F. C., Mahadevan, L., Matsudaira, P. & Weitz, D. A. (2004). Elastic behavior of cross-linked and bundled actin networks. *Science*, **304**, 1301–1305.
19. Chaudhuri, O., Parekh, S. H. & Fletcher, D. A. (2007). Reversible stress softening of actin networks. *Nature*, **445**, 295–298.
20. Semmrich, C., Storz, T., Glaser, J., Merkel, R., Bausch, A. R. & Kroy, K. (2007). Glass transition and rheological redundancy in F-actin solutions. *Proc. Natl Acad. Sci. USA*, **104**, 20199–20203.
21. Kasza, K. E., Rowat, A. C., Liu, J., Angelini, T. E., Brangwynne, C. P., Koenderink, G. H. *et al.* (2007). The cell as a material. *Curr. Opin. Cell Biol.* **19**, 101–107.
22. Janmey, P., Euteneuer, U., Traub, P. & Schliwa, M. (1991). Viscoelastic properties of vimentin compared

with other filamentous biopolymer networks. *J. Cell Biol.* **113**, 155–160.
23. Bousquet, O., Ma, L., Yamada, S., Gu, C., Idei, T., Takahashi, K. *et al.* (2001). The nonhelical tail domain of keratin 14 promotes filament bundling and enhances the mechanical properties of keratin intermediate filaments *in vitro*. *J. Cell Biol.* **155**, 747–754.
24. Coulombe, P. A., Bousquet, O., Ma, L., Yamada, S. & Wirtz, D. (2000). The 'ins' and 'outs' of intermediate filament organization. *Trends Cell Biol.* **10**, 420–428.
25. Ma, L., Xu, J., Coulombe, P. A. & Wirtz, D. (1999). Keratin filament suspensions show unique micromechanical properties. *J. Biol. Chem.* **274**, 19145–19151.
26. Rammensee, S., Janmey, P. A. & Bausch, A. R. (2007). Mechanical and structural properties of *in vitro* neurofilament hydrogels. *Eur. Biophys. J.* **36**, 661–668.
27. Storm, C., Pastore Jennifer, J., MacKintosh, F. C., Lubensky, T. C. & Janmey Paul, A. (2005). Nonlinear elasticity in biological gels. *Nature*, **435**, 191–194.
28. Hofmann, I., Herrmann, H. & Franke, W. W. (1991). Assembly and structure of calcium-induced thick vimentin filaments. *Eur. J. Cell Biol.* **56**, 328–341.
29. Herrmann, H., Haner, M., Brettel, M., Müller, S. A., Goldie, K. N., Fedtke, B. *et al.* (1996). Structure and assembly properties of the intermediate filament protein vimentin: the role of its head, rod and tail domains. *J. Mol. Biol.* **264**, 933–953.
30. Herrmann, H. & Aebi, U. (1999). Intermediate filament assembly: temperature sensitivity and polymorphism. *Cell. Mol. Life Sci.* **55**, 1416–1431.
31. Huiatt, T., Robson, R., Arakawa, N. & Stromer, M. (1980). Desmin from avian smooth muscle. Purification and partial characterization. *J. Biol. Chem.* **255**, 6981–6989.
32. Stromer, M. H., Ritter, M. A., Pang, Y. Y. S. & Robson, R. M. (1987). Effect of cations and temperature on kinetics of desmin assembly. *Biochem. J.* **246**, 75–81.
33. Kirmse, R., Portet, S., Mücke, N., Aebi, U., Herrmann, H. & Langowski, J. (2007). A quantitative kinetic model for the *in vitro* assembly of intermediate filaments from tetrameric vimentin. *J. Biol. Chem.* **282**, 18563–18572.
34. Herrmann, H. & Aebi, U. (2004). Intermediate filaments: molecular structure, assembly mechanism, and integration into functionally distinct intracellular scaffolds. *Annu. Rev. Biochem.* **73**, 749–789.
35. Morse, D. C. (1998). Viscoelasticity of tightly entangled solutions of semiflexible polymers. *Phys. Rev. E*, **58**, R1237–R1240.
36. Gittes, F. & MacKintosh, F. C. (1998). Dynamic shear modulus of a semiflexible polymer network. *Phys. Rev. E*, **58**, R1241–R1244.
37. Willenbacher, N., Oelschlaeger, C., Schopferer, M., Fischer, P., Cardinaux, F. & Scheffold, F. (2007). Broad bandwidth optical and mechanical rheometry of wormlike micelle solutions. *Phys. Rev. Lett.* **99**, 068302–068304.
38. Gisler, T. & Weitz, D. A. (1999). Scaling of the microrheology of semidilute F-actin solutions. *Phys. Rev. Lett.* **82**, 1606.
39. Xu, J., Palmer, A. & Wirtz, D. (1998). Rheology and microrheology of semiflexible polymer solutions: actin filament networks. *Macromolecules*, **31**, 6486–6492.
40. Mücke, N., Kreplak, L., Kirmse, R., Wedig, T., Herrmann, H., Aebi, U. *et al.* (2004). Assessing the flexibility of intermediate filaments by atomic force microscopy. *J. Mol. Biol.* **335**, 1241–1250.
41. Hohenadl, M., Storz, T., Kirpal, H. *et al.* (1999). Desmin filaments studied by quasi-elastic light scattering. *Biophys. J.* **77**, 2199–2209.
42. Steinmetz, M. O., Goldie, K. N. & Aebi, U. (1997). A correlative analysis of actin filament assembly, structure, and dynamics. *J. Cell Biol.* **138**, 559–574.
43. Yanagida, T., Nakase, M., Nishiyama, K. & Oosawa, F. (1984). Direct observation of motion of single F-actin filaments in the presence of myosin. *Nature*, **307**, 58–60.
44. Ott, A., Magnasco, M., Simon, A. & Libchaber, A. (1993). Measurement of the persistence length of polymerized actin using fluorescence microscopy. *Phys. Rev. E*, **48**, R1642–R1645.
45. Gittes, F., Mickey, B., Nettleton, J. & Howard, J. (1993). Flexural rigidity of microtubules and actin filaments measured from thermal fluctuations in shape. *J. Cell Biol.* **120**, 923–934.
46. Isambert, H., Venier, P., Maggs, A. C., Fattoum, A., Kassab, R., Pantaloni, D. *et al.* (1995). Flexibility of actin filaments derived from thermal fluctuations. Effect of bound nucleotide, phalloidin, and muscle regulatory proteins. *J. Biol. Chem.* **270**, 11437–11444.
47. Guzmán, C., Jeney, S., Kreplak, L., Kasas, S., Kulik, A. J., Aebi, U. *et al.* (2006). Exploring the mechanical properties of single vimentin intermediate filaments by atomic force microscopy. *J. Mol. Biol.* **360**, 623–630.
48. Ferry, J. D. (1980). *Viscoelastic Properties of Polymers*, 3rd edit, John Wiley and Sons, New York.
49. Isambert, H. & Maggs, A. C. (1996). Dynamics and rheology of actin solutions. *Macromolecules*, **29**, 1036–1040.
50. Hinner, B., Tempel, M., Sackmann, E., Kroy, K. & Frey, E. (1998). Entanglement, elasticity, and viscous relaxation of actin solutions. *Phys. Rev. Lett.* **81**, 2614–2617.
51. MacKintosh, F. C., Kas, J. & Janmey, P. A. (1995). Elasticity of semiflexible biopolymer networks. *Phys. Rev. Lett.* **75**, 4425–4428.
52. Schmidt, C. F., Bärmann, M., Isenberg, G. & Sackmann, E. (1989). Chain dynamics, mesh size, and diffusive transport in networks of polymerized actin: a quasielastic light scattering and microfluorescence study. *Macromolecules*, **22**, 3638–3649.
53. Gardel, M. L., Valentine, M. T., Crocker, J. C., Bausch, A. R. & Weitz, D. A. (2003). Microrheology of entangled F-actin solutions. *Phys. Rev. Lett.* **91**, *158302.*
54. Onck, P. R., Koeman, T., van Dillen, T. & van der Giessen, E. (2005). Alternative explanation of stiffening in cross-linked semiflexible networks. *Phys. Rev. Lett.* **95**, 178102–178104.
55. Kroy, K. & Glaser, J. (2007). The glassy wormlike chain. *New J. Phys.* 416.
56. Bär, H., Fischer, D., Goudeau, B., Kley, R. A., Clemen, C. S., Vicart, P. *et al.* (2005). Pathogenic effects of a novel heterozygous R350P desmin mutation on the assembly of desmin intermediate filaments *in vivo* and *in vitro*. *Hum. Mol. Genet.* **14**, 1251–1260.
57. Kirschenmann, L. (2003). Aufbau zweier piezoelektrischer Sonden (PRV/PAV) zur Messung der viskoelastischen Eigenschaften weicher Substanzen im Frequenzbereich 0.5 Hz–2 kHz bzw. 0.5 Hz–7 kHz. PhD, Ulm.
58. Crassous, J. J., Regisser, R., Ballauff, M. & Willenbacher, N. (2005). Characterization of the viscoelastic behavior of complex fluids using the piezoelastic axial vibrator. *J. Rheol.* **49**, 851–863.